Multi-Use HF Radar for Arctic Maritime Domain Awareness

Hugh Roarty, Michael Smith, Scott Glenn
Coastal Ocean Observation Laboratory
Rutgers University
New Brunswick, NJ USA
hroarty@marine.rutgers.edu

Chad Whelan, Donald E. Barrick
CODAR Ocean Sensors
Mountain View, CA USA
chad@codar.com

Hank Statscewich, Tom Weingartner
University of Alaska
Fairbanks, AK USA
hank.stats@alaska.edu

***Abstract*— With the increased interest and presence that the U.S. Coast Guard has in the Arctic [1] there is also a rising need for increased Maritime Domain Awareness (MDA) from autonomous sensors in this area. From June through November 2012, University of Alaska, Fairbanks (UAF) deployed and maintained three Long Range SeaSonde@ HF Surface Wave Radars operating in the 5 MHz band and two High Resolution SeaSondes operating in the 25 MHz band to map hourly ocean surface currents in the Chukchi Sea during the summer and fall. With funding from the U.S. Department of Homeland Security (DHS) National Center for Islands, Maritime, and Extreme Environments Security (CIMES), UAF partnered with Rutgers University, a partner in the DHS Center for Secure and Resilient Maritime Commerce (CSR) and CODAR Ocean Sensors to demonstrate multi-use MDA capability of SeaSondes to provide vessel detections simultaneously with surface current maps near Barrow, Alaska. The Arctic region poses challenges to HF Radar vessel detection including: remote locations requiring specialized shelter, power and communications; extreme weather; the presence of ice floes, which have their own Doppler echoes in addition to sea clutter; and a different radio environment with auroral influences. Vessel detection results are shown with corresponding AIS data, the effect of diurnal ionosphere activity on HF Doppler spectra is shown and the performance of the UAF remote power module (RPM) is discussed.**

Keywords—remote sensing, high frequency radar, ocean currents, vessel detection, maritime domain awareness

I. INTRODUCTION

From June through November 2012, the University of Alaska Fairbanks deployed and maintained three Long Range SeaSondes operating in the 5 MHz band (Figure 1) and two High Resolution SeaSondes operating in the 25 MHz band to monitor hourly 2-D surface currents in the Chukchi Sea during the summer and fall.

This project was sponsored by the United States Department of Homeland Security's Center for Island, Maritime, and Extreme Environment Security.

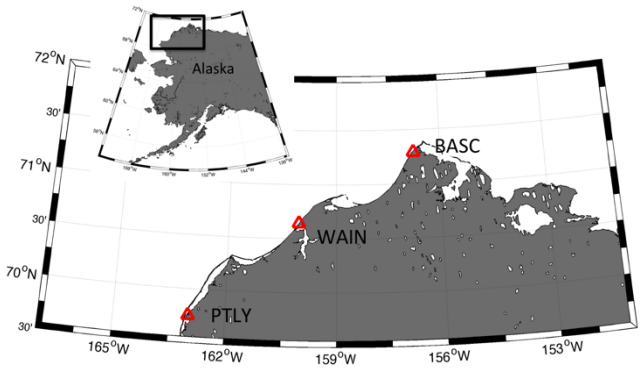

Figure 1: Map of the study area along the north slope of Alaska. The three 5 MHz radars are indicated by the red triangles with the site code for each station Point Barrow (BASC), Wainwright (WAIN) and Point Lay (PTLY).

In addition to the surface current measurements, the radar system at Point Barrow (BASC) was outfitted with real time vessel detection software. Vessels detected by the radar ranged in size from tug boats 23 m in length to ice breakers more than 110 m in length. Detection statistics on three observables (range, range rate and bearing) were presented along with vessel tracks [2]. The goal of this paper is to characterize two additional measurements that were made by the radar during this experiment.. The second measurement was that of the environmental noise in the Arctic at the High Frequency radio band. Lastly, the authors would like to report on the performance of the Remote Power Module, which was used to power one of the radar stations during the experiment.

II. RADAR DETECTIONS

The radar at Point Barrow generated vessel detections from August 15 to October 31, 2012. Daily plots were made of the vessel detection data and ship tracks could clearly be seen in the plots. For instance Figure 2 shows the detections for September 10, 2012. You can see a vessel approaching the radar in the range panel between 00:00 and

03:00 UTC and another one between 06:00 and 09:00. There are several vessels passing by the radar in the 5 to 20 km range throughout the day.

Automatic Identification System (AIS) data was used to verify the vessel detections. An example of this is given in Figure 3, where the radar detections are the different colored dots and the track of the Coast Guard icebreaker Healy (Figure 4) from AIS is the aqua line. The radar was able to detect the icebreaker out to 81 km. The radar was not able to detect the vessel when it was stationary with zero Doppler shift, which makes sense for a Doppler radar. The radar detection algorithm also had difficulty in detecting the vessel when it was accelerating causing the returned energy to be spread over several Doppler bins. This will require a reexamination of the detection algorithm to account for this vessel behavior.

Figure 5 gives another example of a vessel detected by the radar. This time the vessel was quite smaller, the tugboat Nokea (Figure 6). Again the radar detection algorithm had difficulty detecting the vessel when it was accelerating. The vessel was detected for 19 hours as it operated in front of the radar. This is one of the longest detection records we have recorded with the SeaSonde.

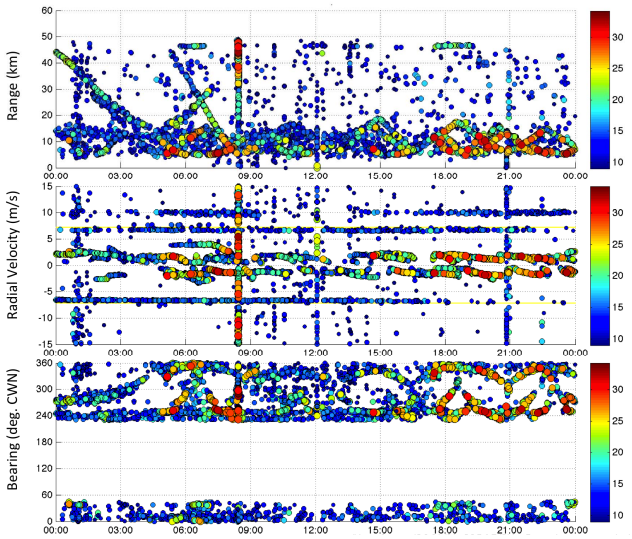

Figure 2: Plot of vessel detection data for September 10, 2012. The top panel shows target range (km); the middle panel shows target radial velocity (m/s) and the bottom panel shows target bearing (degrees clockwise north). The colorbar denotes the signal strength (dB).

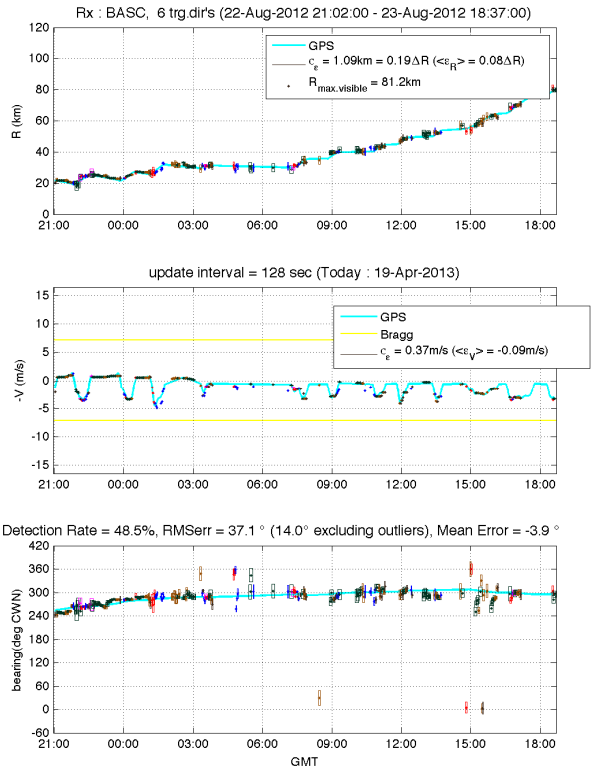

Figure 3: Radar detections of the icebreaker Healy (dots) overlaid on the AIS track of the vessel (aqua lines). The panels are the same as Figure 2.

Figure 4: Picture of the US Coast Guard icebreaker Healy.

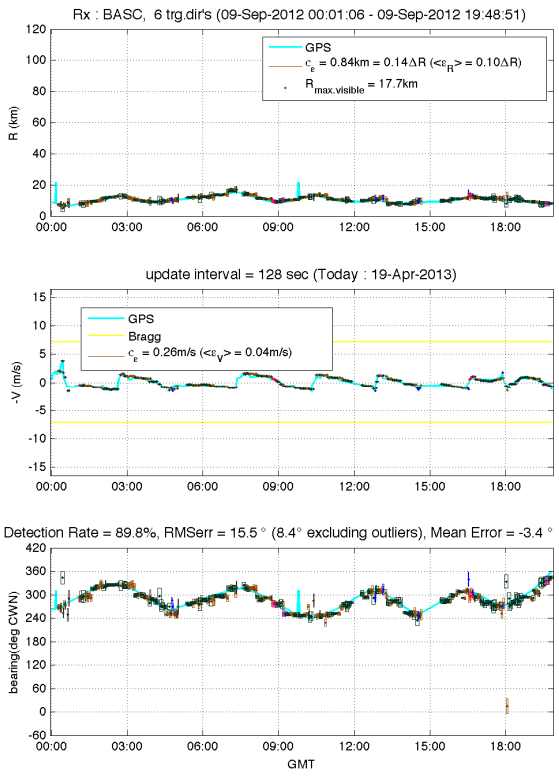

Figure 5: Radar detections of the tug boat Nokea (dots) overlaid on the AIS track of the vessel (aqua lines). The panels are the same as Figure 2.

Figure 6: Picture of the tugboat Nokea.

III. HIGH FREQUENCY NOISE ENVIRONMENT

The SeaSonde provides an estimate of the High Frequency noise environment as part of its diagnostic data output. These data were plotted and analyzed across all three long-range systems. The receive antenna of the SeaSonde consists of two directionally dependent cross loops (Channels 1 and 2) and an omnidirectional monopole (Channel 3)[3, 4]. The maximum range and noise floor measurements for each of the channels are saved in radial diagnostic files (.rdt). The noise floor diagnostic data from the 5 MHz system at Point Barrow is plotted in Figure **7**.

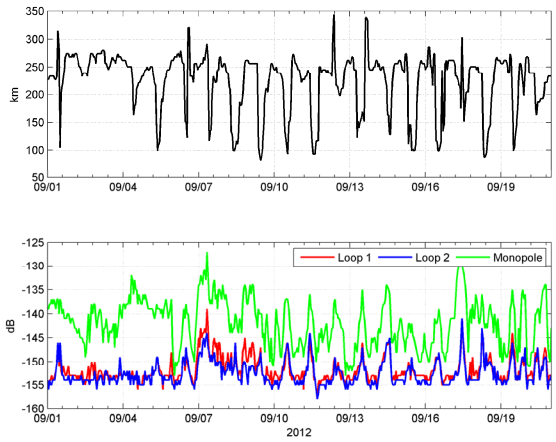

Figure 7: Time series plot of maximum range (top panel) and the noise floor data (bottom panel) for Loop 1 (red) Loop 2 (blue) and Loop 3 (green) at the BASC site from September 1, 2012 until September 21, 2012.

The maximum range time series clearly shows a diurnal cycle, which is related to temporal variations in the ionosphere driven primarily by solar radiation [6]. As the noise floor data increases across the three channels of the receive antenna, the maximum range decreases from approximately 340 km to 82 km. The mean noise floor measurements for each channel are binned by time of day in Figure **8**. The reduction in range is strongly correlated to the time of day, with the highest noise occurring at 11:00 UTC or 3:00 am local time. This bin averaging was repeated for channel 3 at the two other 5 MHz systems (WAIN and PTLY) and is shown in Figure 9. They also display a clear diurnal signal. The phasing of PTLY agrees with BASC, however the peak for WAIN arrives three hours later at 6:00 am local time. The noise floor data from each of the sites is summarized in Table 1. The noise floor is highest on Channel 3 for all three sites and this channel also has the highest variance of all the channels.

A time series of the global Kp-index and minimum heights of the E and F layers of the ionosphere are shown in Figure 10. The Kp index quantifies disturbances in the earth's magnetic field and is measured on a scale of 0 through 9. Kp values of 5 or greater are considered geomagnetic storms, which disturb the F-layer of the ionosphere resulting in significant degradation of radio wave propagation [5]. During the period of Sept. 1 – Sept. 21, 2012 the Kp index was 5 or greater 14% of the time.

Table 1: Average and standard deviation of the noise floor measurements of the long-range SeaSonde at the three locations in Alaska along with the number of data points for each site. The average for all three stations is shown as the bottom row.

	Mean(Ch. 1)	Mean(Ch. 2)	Mean(Ch. 3)	Std(Ch. 1)	Std(Ch. 2)	Std(Ch. 3)	N
BASC	-152	-152	-144	3.5	3.8	6.2	6300
WAIN	-149	-149	-146	4.5	5.1	9.3	7000
PTLY	-147	-154	-141	4.3	4.5	6.5	5700
Average	-149	-152	-144	4	4	7	6333

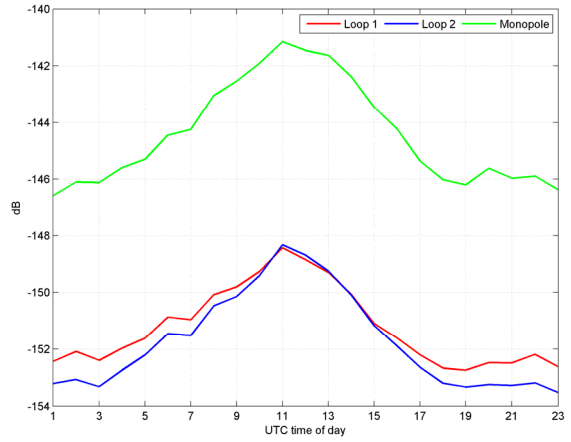

Figure 8: Mean noise floor measurement binned by time of day for the BASC radar site.

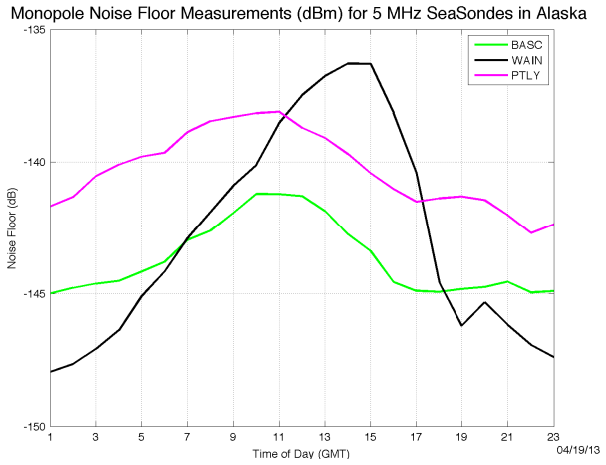

Figure 9: Mean noise floor measurements for Channel 3 binned by time of day for all three 5 MHz SeaSondes.

When the radar signals encounter interference layers characteristic of high-latitude geomagnetic storms, they return intense echoes spread across all Doppler cells. They also extend over more distant ranges, from the lowest range outward. This is unlike overhead ionospheric reflections that are seen at lower latitudes, which block echoes from only a few range cells. Consequently, not all of the echo is totally reflected from the first layer, but comes from volumetrically distributed echoes from rapidly moving particles extending past that point in range, making it impossible to see peaks which correspond to reflected ocean waves on the horizon that extend beyond that range.

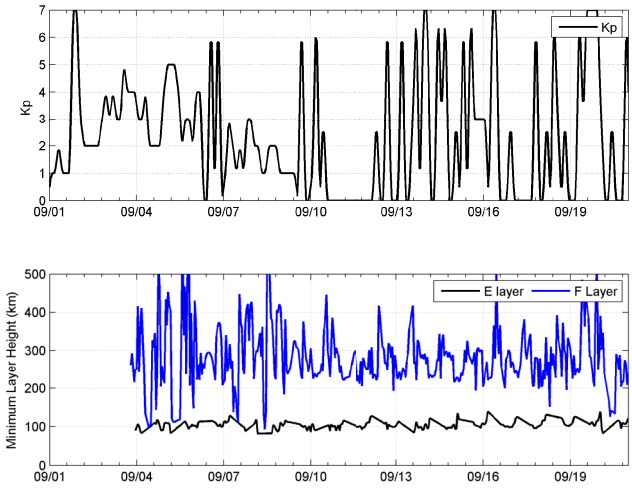

Figure 10: Time series plot of the planetary Kp index (top panel) and height of the ionosphere E and F layers (bottom panel) collected from ionosonde measurements at Gakona, Alaska.

Although the transmit antenna has a minimum in the overhead direction, energy is still transmitted in that direction. This white noise effectively blocks any reflections from any further out than 80 km, cutting the working range of the HFR by one-third. An example of the effects of a geomagnetic storm are shown in Figure 11, the large band of white noise occurring at 85 km range blocks all sea echo from that point onward, just a few hours later, ocean echoes are observed out to 240 km with little interference. The ionosphere at high latitudes effectively limits vessel detection to 80 km range during nighttime hours.

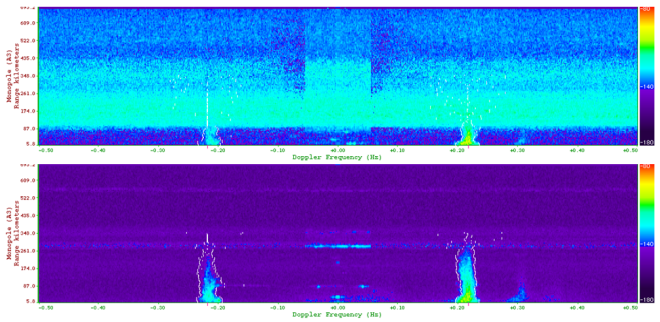

Figure 11: Contour map of monopole spectra collected at the BASC site at 11:00 UTC (top) and 22:00 UTC (bottom) September 9, 2012.

IV. Remote Power Module

A. Introduction

The Remote Power Module [6] (herein referred to as the RPM) deployed at Point Barrow Alaska was designed and deployed by the University of Alaska Fairbanks (UAF). A picture of the RPM is shown in Figure 12. The RPM's primary purpose is to support High Frequency (HF) Radar used to measure ocean currents; in addition the RPM also

supports a number of ancillary sensors such a meteorological station (wind speed and direction, air temperature, and solar radiation) and Automatic Identification System (AIS) base stations. All data is telemetered to Fairbanks in near real time. The RPM is a fully–automated, renewable (solar and wind) hybrid power station designed for arctic and sub-arctic maritime environments. It provides a remotely deployable platform with a compact footprint amenable to the difficult permitting requirements in many coastal areas. A climate controlled shelter houses the high-frequency radar electronics, communications equipment and electrical system components of the power plant [9].

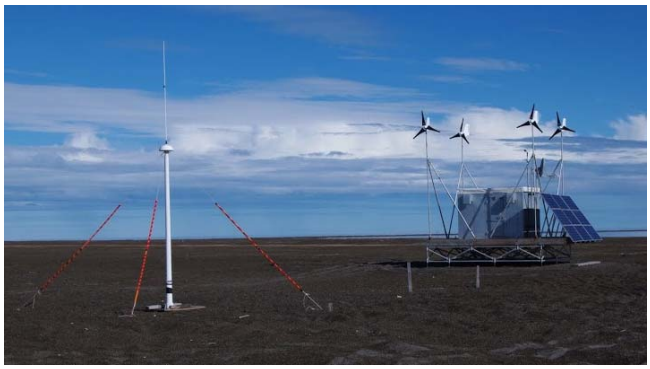

Figure 12: Picture of the HF Radar receive antenna (left) and the Remote Power Module as deployed at Point Barrow, Alaska.

The system is designed to reduce operating costs through reliance on renewable energy. Using fossil fuel based generators as a primary power source is costly due to frequent maintenance requirements, limited life expectancies and ongoing logistics and fuel costs. The total power requirements of the electronics are approximately 11 Kilowatt-hours per day. The RPM is portable enough to be installed and serviced from small cargo planes, boats, four-wheelers or snow machines with trailers.

B. Performance of the RPM

The RPM supplied the necessary power to keep the HF Radar, meteorological station, AIS base station and satellite modem (necessary for real-time data telemetry) operating from July 10, 2012 through December 7, 2012 when the unit was shut down and winterized. The majority of vessel detections were collected in August through mid-October 2012 so our discussion of the data collected at the RPM will focus on that time period. A time series of wind speed, incoming solar radiation and air temperature (Figure **13**) shows that the power module was subjected to high winds with mean wind speed over the period at 6.6 meter per second (12 knots) and gale winds (>16 m/s) observed on September 17. In addition, available solar radiation peaked in early August and decreased rapidly after the mid-September autumnal equinox. The mean air temperature was 3.5° Celsius, with maximum temperatures of 14° C in August and a minimum of -5° C in October.

The RPM is powered by four wind turbines rated at 600 watts each, photovoltaic array rated at 1.8 kilowatts and a backup 10 KW generator. All power generated is stored in a 2,700 amp-hour battery bank. In 2012, there was no need for the backup generator as all power necessary for the HFR equipment was supplied through renewable resources (solar and wind). A time series of battery bank voltage shows that the mean voltage hovered between 24.5 and 26.5 VDC with a mean voltage of 25.1 VDC (Figure **13**). These voltages correspond to very healthy fluctuations of 75% - 100% state of charge of the bank. The instantaneous current produced from the wind and solar arrays varied between 0 to 1.8 kilowatts, with 72% of total power produced delivered from the wind turbines.

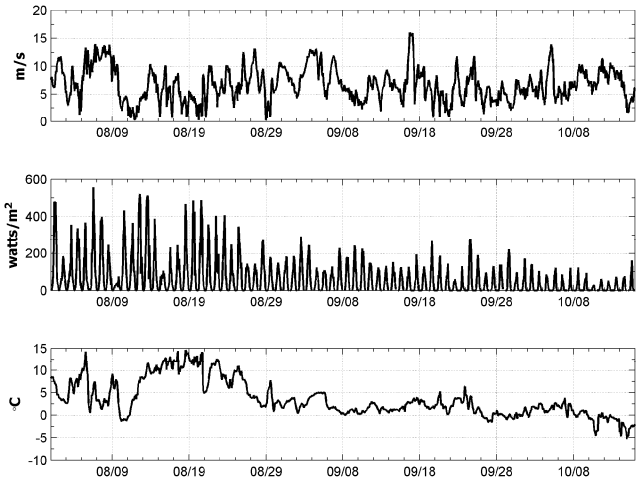

Figure 13**: Wind speed (top panel) solar radiation (middle) and ambient air temperature (bottom) collected at the RPM for the period July 10 – October 16, 2012.**

V. CONCLUSIONS

The 5 MHz SeaSonde HF radar was operated at three locations along the North Slope of Alaska for a period of six months in the summer/fall of 2012. The radar at Point Barrow made simultaneous measurements of surface currents and detected the location and radial velocity of several vessels that passed in front of the radar. The radar estimated the radar cross section of these vessels. We observed a slight correlation between RCS and vessel length. The noise environment in the HF band was characterized using the noise measurement of the SeaSonde. Finally, a remote power module was demonstrated to deliver consistent power for the SeaSonde in this remote environment. All three of these measurements will help provide information to the United States Coast Guard for additional maritime domain awareness in the Arctic. The HF radar can provide surface current measurements for oil spill response and environmental monitoring, vessel detection and classification information for maritime security.

ACKNOWLEDGMENTS

This material is based on work supported by the U.S. Department of Homeland Security under Award No. 2008-ST-061-ML0001. The views and conclusions contained in this document are those of the authors and should not be interpreted as necessarily representing the official policies,

either expressed or implied, of the U.S. Department of Homeland Security.

REFERENCES

[1] K. Johnson. (2012, Date) For Coast Guard Patrol North of Alaska, Much to Learn in a Remote New Place. Magazine.

[2] H. Roarty, M. Smith, S. Glenn, D. E. Barrick, C. Whelan, E. Page, H. Statscewich, and T. Weingartner, "Expanding Maritime Domain Awareness Capabilities in the Arctic: High Frequency Radar Vessel Tracking," in *Radar Conference, 2013. RADARCON 13. Proceedings of the 2013 IEEE*, 2013.

[3] B. J. Lipa and D. E. Barrick, "Least-squares methods for the extraction of surface currents from CODAR cross-loop data: application at ARSLOE," *IEEE Journal of Oceanic Engineering,* vol. OE-8, pp. 226-253, 1983.

[4] J. T. Kohut and S. M. Glenn, "Improving HF Radar Surface Current Measurements with Measured Antenna Beam Patterns," *Journal of Atmospheric and Oceanic Technology,* vol. 20, pp. 1303-1316, September 01, 2003 2003.

[5] C. C. Teague, "Ionospheric Effects on Coastal Radar Systems," *Proceedings of the Radiowave Oceanography Workshop,* vol. Timberline, OR, 2001.

[6] H. Statscewich, T. Weingartner, S. Danielsen, B. Grinau, G. Egan, and J. Timm, "A High-Latitude Modular Autonomous Power, Control, and Communication System for Application to High-Frequency Surface Current Mapping Radars," *Marine Technology Society Journal,* vol. 45, pp. 59-68, 2011.